
SPECTROSCOPY AND PHYSICS
OF ATOMS AND MOLECULES

Infrared Spectra of the Halothane–Trimethylamine Complex in Liquefied Krypton

S. M. Melikova^a and K. S. Rutkowski^{a,*}

^a Saint Petersburg State University, St. Petersburg, 199034 Russia

*e-mail: k.rutkovsky@spbu.ru

Received December 3, 2020; revised December 3, 2020; accepted December 15, 2020

Abstract—The IR absorption spectra of solutions of mixtures of halothane ($C_2HBrClF_3$) and trimethylamine ($(CD_3)_3N$) in liquefied krypton were obtained and analyzed. Bands assigned to weak hydrogen-bonded complexes have been identified. In a series of temperature experiments on the change in the integral intensities of the bands of monomers and complexes, the enthalpy of formation of complexes was estimated. An extremely strong increase in the intensity of the second-order bands attributed to the first overtone of bending CH vibrations of halothane was found. The effect is determined by strong anharmonic interactions of a resonant nature (Fermi resonance and Darling–Dennison resonance). The results of ab initio calculations reproduce the experimentally observed effects.

Keywords: IR spectra of cryosolutions, liquid Kr, halothane, hydrogen bond, ab initio calculations

DOI: 10.1134/S0030400X21040159

INTRODUCTION

The ability of halothane (Halothane, $C_2HBrClF_3$) to interact with a target molecule having regions of increased electron density is mainly determined by the presence of a CH group. Possessing the properties of a weak donor, this anesthetic molecule can participate in the formation of complexes with hydrogen bonding (HB). This is confirmed by examples of interactions of halothane with methyl fluoride (FCD_3) [1], dimethyl ether ($O(CD_3)_2$) [2], acetone ($OC(CD_3)_2$) [3], and benzene [4]. By the nature of the spectroscopic changes detected during the formation of complexes with weak HB, this anesthetic can be attributed to systems with the so-called “blue” or “atypical” HB [1–3]. When such CH donors interact with increasingly strong proton acceptors, a transition from a high-frequency shift to a “normal” low-frequency shift, as well as a noticeable increase in the intensity of the CH stretch band, will be expected. This character of changes in spectroscopic parameters is confirmed both experimentally and by a number of calculations [5–10].

In this work, using the IR absorption spectra of cryosolutions, we studied the features of the formation of complexes with the participation of halothane as a CH donor and trimethylamine (TMA) as a strong nitrogen-containing proton acceptor. The experiments were carried out with small additions of TMA. It is natural to assume that in the system under consideration only heterodimers with characteristics close to

the “normal” HB will be formed. The measurement results are analyzed using ab initio calculations carried out using the GAUSSIAN quantum-chemical package. The observed spectroscopic effects are considered taking into account the strong anharmonic interactions of the resonance type.

EXPERIMENTAL AND CALCULATION TECHNIQUE

The IR absorption spectra of mixtures of halothane with TMA were recorded in the range 800–4000 cm^{-1} with a resolution of 0.5 cm^{-1} on a Nicolet 6700 Fourier spectrometer. Liquefied krypton (Kr) was used as a solvent in the temperature range of 118–155 K. The halothane and TMA concentrations were 5×10^{16} – 10^{17} mol/cm³. In order to avoid overlapping of the absorption bands of the proton donor and acceptor in the region of stretching vibrations CH of halothane, a deuterated TMA-D9 ($(CD_3)_3N$) sample was used. The measurements were carried out in an optical cryostat cooled with liquid nitrogen. The setting of the required temperature was carried out both by dosing liquid nitrogen and by heaters placed in the body of a copper radiator. The temperature with an error of 3 K was controlled by the vapor pressure over the liquid solution. The 7 cm long stainless steel optical cryostat cell is equipped with BaF_2 windows sealed with indium gaskets. It was located in the body of a copper radiator attached to a vessel with liquid nitrogen. The enthalpy of formation ΔH_T was estimated from temperature

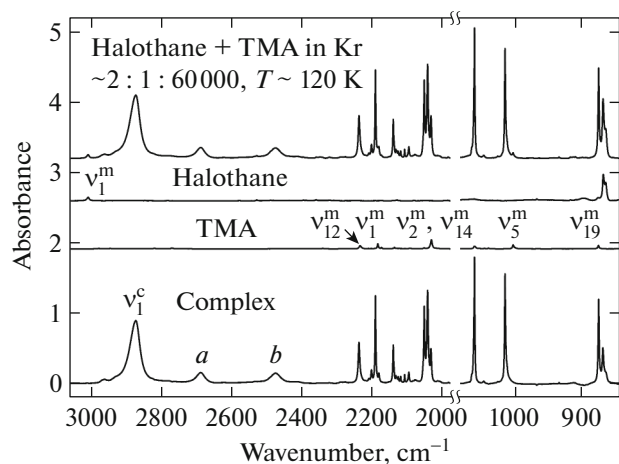


Fig. 1. Infrared spectrum of a mixture of $C_2HBrClF_3$ with $(CD_3)_3N$ in liquid Kr—upper spectrum; the result of high-lighting the bands of the complex is the lower spectrum.

measurements of the integrated intensities of the absorption bands assigned to the monomers and the complex. In this case, the correction for the temperature change in the krypton density was taken into account which is ~ 0.6 kJ/mol [11].

The calculations were performed using the GAUSSIAN16 Rev. A.03 quantum mechanical package [12]. The results were obtained in the second-order approximation of the Møller–Plesset perturbation theory (MP2) [13] as well as using the density functional theory (DFT) [14]. The bulk of the calculations (in the harmonic approximation, and in some cases, taking into account anharmonic effects), were carried out with the valence-split Pople basis sets, including polarization and diffuse functions: 6-31++G(d,p) and 6-311++G(d,p). The choice of the method and bases was made based on a compromise between the reproducibility of the detected spectroscopic effects and the available computer resources. The geometry, interaction energy and frequencies of normal vibrations of the complex were obtained taking into account the basis superposition error (BSSE) [15, 16]. Anharmonic effects were estimated both using the output data of the calculation in the GAUSSIAN16 environment and by directly solving the secular equation, including the Fermi and Darling–Dennison (D–D) resonances [17].

MEASUREMENT RESULTS

In Fig. 1 the region of the $\nu_1(CH)$ stretching vibration band of halothane, the region of the $\nu(CD_3)$ TMA stretching vibration bands (left side) and some bending vibrations (right side) for a mixture of $C_2HBrClF_3$ with $(CD_3)_3N$ in liquid krypton at 120 K are presented. The lower part of the figure shows the bands of the complex. They were obtained by subtracting the bands

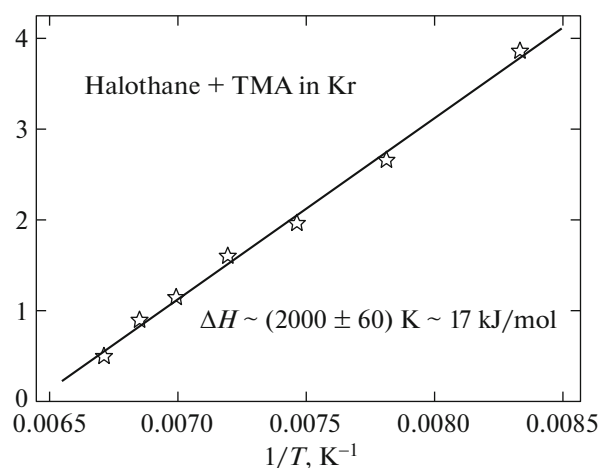


Fig. 2. Van Hoff's dependence ($\ln K = -\Delta H_T/RT + \Delta S/R$, R is the universal gas constant, ΔS is the change in entropy during the formation of a complex); the ordinate is the natural logarithm of the ratio of the area of the TMA band in the complex to the product of the areas of the bands of monomers (TMA and halothane).

of monomers from the bands with the selected coefficients. The experiment showed that the intensity of the bands is redistributed in favor of the bands of monomers with increasing temperature of the solution. The complex formation leads to a significant increase in the intensity of the $\nu_1(CH)$ stretching vibration band of halothane. From a series of temperature and concentration measurements, it follows that it is many tens of times. A strong broadening of this band (from 6 to 35 cm^{-1}) is also noted, as well as a shift of the maximum towards the low-frequency side by $\Delta\nu^{c-m} \sim -136$ cm^{-1} . The absolute value of the shift decreases slightly with increasing solution temperature in liquid krypton. The recorded high-frequency shift of the $\nu(CD_3)$ TMA stretching vibration bands is small. At $T \sim 120$ K, it is $1-3$ cm^{-1} . The high-frequency shift of the TMA bending vibration bands is also small.

On the left side of the Tables 1 and 2, the most characteristic measurement results for individual bands of monomers and the complex, obtained at $T \sim 120$ K, are presented. For TMA, the literature data obtained in the gas phase are also given [18]. The bands are numbered in decreasing order of the wave number of normal vibrations of free halothane. For TMA, the numbering of bands proposed in [18] is adopted. Based on the results of temperature measurements of the integral intensities of the fundamental bands of monomers and the complex in liquid krypton ($T \sim 120-155$ K), the Van Hoff dependences were plotted ($\ln K = -\Delta H_T/RT + \Delta S/R$, R is the universal gas constant, ΔS is the change in entropy complex formation) and the enthalpy of formation of the ΔH_T complex was estimated. In Fig. 2 an example of such a dependence when choosing the TMA vibration band

Table 1. Measured and calculated (MP2/6-311++G(d,p)) spectroscopic parameters of individual bands of halothane (C₂HBrClF₃) and TMA ((CD₃)₃N)

Assignment		Gas	Solution in Kr, 120 K			MP2/6-311++G(d,p)			Fermi + D–D	
C ₂ HBrClF ₃ ; C ₁		ν^m	ν^m	$2\Gamma^m$	S_{rel}	$\omega^m (A^m)$	$\nu^m (A^m)$	A_{rel}	$\nu^m (A^m)$	A_{rel}
ν_1	$\nu(\text{CH})$	3017.7	3007.5	8.5	1(3.4)	3185 (3.0)	3052	1(3.1)	3065	1
$2\nu_2$		—	—	—	—	2731 (0)	2655 (0.08)	0.03	2770 (0.11)	0.04
$2\nu_3$		—	—	—	—	2612 (0)	2544 (0.6)	0.2	2602 (~0)	0
$2\nu_4$		—	—	—	—	2518 (0)	2452 (0.2)	0.07	2529 (0.24)	0.08
ν_2	$\delta(\text{CCH})$	~1314	1311.1	~1.6	15	1365 (80)	1332 (65)	22		
ν_3	$\nu(\text{CC}) + \delta(\text{CCH})$	~1277	1269	~1.5	35	1306 (197)	1276 (176)	59		
ν_4	$\gamma(\text{CCH})$	—	1217	~2	3	1259 (15)	1235 (20)	7		
$\nu_7 \text{Cl}^{35}$	$\nu^s(\text{CC}) + \nu^s(\text{CF}_3)$	~868	862.6	3.0 2.8	3 4	890 (37)	874 (32)	11		
$\nu_7 \text{Cl}^{37}$									833.2	
$\nu_8 \text{Cl}^{35}$	$\nu(\text{CCl})$		812.5		8 6	849 (74)	831 (59)	20		
$\nu_8 \text{Cl}^{37}$									810.7	
(CD ₃) ₃ N; C _{3v}										
$\nu_{12}(\text{E})$	$\nu_{as}'' \text{CD}_3$	2236.8 [18]	2232.7	~7	1	2350 (18.2)	2274 (12.2)	1		
ν_1 (A ₁)	$\nu_{as}' \text{CD}_3$	2185.9 [18]	2182.0	~3.5	0.9	2288 (55)	2222 (30)	1.2		
ν_5 (A ₁)	$\rho' \text{CD}_3$	1005.0 [18]	1003.8	~2.6	0.7	1038 (36)	1012 (33)	1.4		
$\nu_{19}(\text{E})$	$\rho' \text{CD}_3$	875.2 [18]	873.8	~2.5	0.5	899 (8.2)	883 (9.2)	0.8		

Designations: ν^m (ω^m)—wave number (ω —harmonic) of the vibrational band of the monomer at the maximum in cm^{-1} ; $2\Gamma^m$ is the bandwidth at half maximum in cm^{-1} ; A is the absolute intensity in km/mol ; A_{rel} (S_{rel}) is the relative intensity (area) of the band; the intensity (area) of the $\nu_1(\nu_{12})$ band of halothane (TMA) is taken as unity.

in the complex at $\sim 1016 \text{ cm}^{-1}$ and monomer bands at $\sim 1004 \text{ cm}^{-1}$ for TMA and at $\sim 3007 \text{ cm}^{-1}$ for halothane is presented. The enthalpy of formation, obtained from the slopes of the individual graphs, taking into account the temperature change in the density of the liquid, is in the range from -17 to $-19 \text{ kJ}/\text{mol}$ in liquid krypton. The average value of the enthalpy of formation of the complex of halothane with TMA in liquid krypton is ~ 18 (1) kJ/mol .

CALCULATION RESULTS AND DISCUSSION

Under the conditions of cryosolutions, as well as in the gas phase, a staggered configuration is a stable conformer of halothane [2, 19]. When searching for minima on the potential energy surface (PES) of a system consisting of interacting halothane and TMA, a structure was found that corresponds to the real minimum (the absence of imaginary frequencies in the calculations). It is shown in Fig. 3 (together with dihedral angle D_7 (N10–C9–C2–C1)). A TMA molecule

belonging to the C_{3v} symmetry group with three symmetrically arranged CD₃ groups attached through a single bond to the nitrogen atom can undergo hindered rotation in a complex stabilized by the CH \cdots N hydrogen bond. This natural assumption is confirmed by single point calculations when scanning the dihedral angle D_7 (N10–C9–C2–C1) within 360° . The result of such a scan, performed in the MP2/6-31++G(d,p) approximation, with optimization for the rest of the variables (relaxed scans) is shown in Fig. 4. Indeed, the height of the barrier between successive (practically equivalent) minima does not exceed 50 K ($\sim 35 \text{ cm}^{-1}$).

Then the resulting structure was optimized using the triple-zeta basis 6-311++G(d,p). Next, the spectroscopic parameters of the monomers and heterodimer were calculated. A comparison is made of the results obtained in the framework of the MP2 perturbation theory and using popular density functionals with empirical dispersion interactions (APFD, WB97xd, B3LYP with empirical dispersion = gd3). It

Table 2. Measured and calculated (MP2/6-311++G(d,p)) spectroscopic parameters of individual bands of the $(\text{CD}_3)_3\text{n...HC}_2\text{BrClF}_3$ complex

Assignment	Solution in Kr, 120 K			MP2/6-311++ G(d,p) anharmonic (4 modes)			Fermi + D–D	
	$\nu^c (S^c; S_{\text{rel}}^c)$	$2\Gamma^c$	$\Delta\nu^{c-m}$	$\omega^c (A^c)$	$\Delta\omega^{c-m}$	$\nu^c (A^c; A_{\text{rel}}^c)$	$\nu^c (A^c; A_{\text{rel}}^c)$	$\Delta\nu^{c-m}$
$\text{C}_2\text{HBrClF}_3$								
ν_1	2871.5 (40; 1)	35	–136	3037 (358)	–148	2933 (239; 1)	2926 (261; 1)	–139
$2\nu_2$	2686.2 (6; 0.15)	~32	–	2849 (0)	–	2727 (82; 0.3)	2768 (32; 0.12)	–2
$2\nu_4$	2472 (9.6; 0.24)	~35	–	2680 (0)	–	2571 (41; 0.17)	2536 (60; 0.23)	+7
ν_2	1352	~20	+41	1424 (25)	+59	1390 (20)		+58
ν_3	1272		+3	1310 (223)	+4	1280 (187)		+4
ν_4	1309		+92	1340 (24)	+81	1307 (28)		+72
ν_7	866.9	2.9	+0.7	892 (25)	+2	–		
TMA								
ν_{12}	2235.7	~5	+3	2352 (23)	+2	–		
ν_1	2188.9	~3	+6.9	2297 (21)	+9	–		
ν_5	1016.3	~3	+12.5	1050 (43)	+12	–		
ν_{19}	873.5	~2	–0.3	898 (20)	–1	–		

Designations: A^c —absolute intensity in km/mol ; $\nu^c (\omega^c)$ —wavenumber (ω —harmonic) of the vibrational band of the complex at the maximum in cm^{-1} ; $2\Gamma^c$ is the bandwidth at half maximum in cm^{-1} ; $\Delta\nu^{c-m} (\Delta\omega^{c-m})$ is the shift of the wavenumber during complex formation; for convenience of comparison, the numbering of the bands of the components of the complex is chosen to coincide with the numbering of the bands of free molecules.

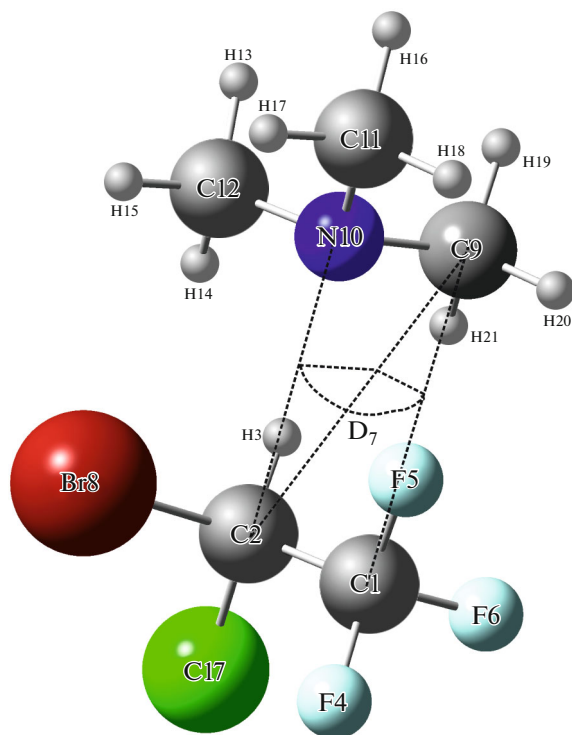


Fig. 3. Equilibrium geometry of the complex found in the calculations MP2(FC)/6-311++G(d,p) with dihedral angle D_7 (N10–C9–C2–C1), which determines the orientation of TMA relative to halothane in the complex.

is noted that although the DFT methods lead to a good agreement between the values of the measured and calculated wavenumbers of individual normal vibrations, the approach based on the second order of the perturbation theory (MP2), at overestimated absolute values of frequencies, principally better describes the relative changes in spectroscopic parameters during the formation of a complex. This is especially true for anharmonic resonance effects, which determine the nature of changes in the region of the $\nu_1(\text{CH})$ stretching vibration band of halothane. On the right side of the Tables 1 and 2, the results of harmonic and anharmonic calculations performed at the MP2/6-311++G(d,p) level with allowance for the superposition basis error (with the option “counterpoise = 2” in the GAUSSIAN package) are presented. It should be noted that the demand for anharmonic calculations at the MP2/6-311++G(d,p) level to computer resources is growing. Most importantly, such a complete anharmonic analysis leads to a series of physically absurd results (for example, the appearance of imaginary frequencies even in the wavenumber region of the order of 600 cm^{-1} , an unexpected multiple increase in the intensity of individual first-order bands, etc.). Since the main experimentally observed effect is associated with the appearance of wide intense satellites on the low-frequency side of the band of the $\nu_1^c(\text{CH})$ complex, it was quite reasonable to restrict ourselves to the

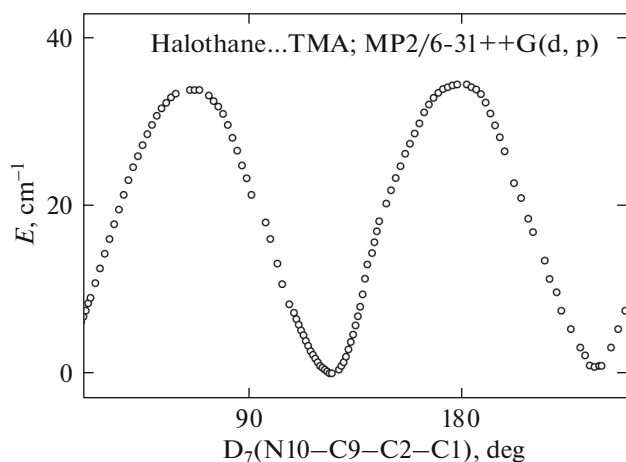


Fig. 4. Result of scanning (MP2(FC)/6-31++G(d,p)) along the dihedral angle D_7 with optimization for the rest of the complex variables (relaxed scan with respect to the dihedral angle D_7).

truncated form of anharmonic calculations, taking into account only four modes of halothane, potentially participating in resonance interactions. In accordance with the classification given in Tables 1 and 2, they are ν_1 , ν_2 , ν_3 , ν_4 . It should be noted that the formation of a complex leads to an increase in the wave number of modes ν_2 , ν_3 , ν_4 , which is especially significant in the case of the last mode ν_4 , which corresponds to the bending vibration $\gamma(\text{CCH})$. As a result, the main bands ν_3 and ν_4 in the complex change places.

$$\begin{array}{l}
 \langle 1000 | \\
 \langle 0200 | \\
 \langle 0110 | \\
 \langle 0101 | \\
 \langle 0020 | \\
 \langle 0011 | \\
 \langle 0002 |
 \end{array}
 \left| \begin{array}{ccccccc}
 E_1^0 & W_{1_22} & W_{1_23} & W_{1_24} & W_{1_33} & W_{1_34} & W_{1_44} \\
 & E_2^0 & W_{22_23} & W_{22_24} & W_{22_33} & 0 & W_{22_44} \\
 & & E_3^0 & W_{23_24} & W_{33_23} & W_{23_34} & 0 \\
 & & & E_4^0 & 0 & W_{24_34} & W_{44_24} \\
 & & & & E_5^0 & W_{33_34} & W_{33_44} \\
 & & & & & E_6^0 & W_{44_34} \\
 & & & & & & E_7^0
 \end{array} \right. \cdot \quad (1)$$

Here, the diagonal terms represent the unperturbed interaction frequencies of the states represented in the left column. They are calculated using standard formulas (for example, [20]) using the following set of spectroscopic parameters: harmonic frequencies ω_1 , cubic α_{ijk} , and quartic β_{ijkl} constants, as well as unperturbed anharmonic constants x_{ik}^0 (anharmonic constants, from which resonance terms are excluded). In Table 3 the values of these parameters obtained in calculations at the level of MP2/6-311++G(d,p) (with the option anharm, select 4 anharmonic modes) for

free halothane and for the halothane-TMA complex are presented.

Thus, the results of the calculation and spectroscopic experiment demonstrate a strong (almost 100-fold) increase in the intensity and a low-frequency shift of the ν_1 band of the C–H stretching vibration of halothane. A multiple (~ 4 times) broadening of this band is also observed. The noted effects are characteristic of medium-strength hydrogen bonds. The formation of the complex is also accompanied by the appearance of rather intense broadened low-frequency satellites, which are assigned to the $2\nu_2$ and $2\nu_4$ overtones of the bending vibrations $\delta(\text{CCH})$ and $\gamma(\text{CCH})$. This interpretation is confirmed by the results of calculations in the anharmonic approximation. It should be noted that the result extracted directly from the file (middle part of Table 2) reflects the appearance of satellites detected in the experiment. But it strongly (twofold) overestimates the relative intensity of the first band, ascribed to the $2\nu_2$ overtone.

As a result of the analysis of the results of the GAUSSIAN 16 calculation, it was found that for the considered region only one Fermi resonance $\nu_1/2\nu_2$, was taken into account. The rest of the anharmonic interactions are taken into account approximately according to the perturbation theory. The result can be substantially corrected by considering all interactions: $\nu_1/2\nu_2/(\nu_2 + \nu_4)/(\nu_2 + \nu_3)/2\nu_4/(\nu_4 + \nu_3)/2\nu_3$, containing both Fermi resonances and Darling–Dennison resonances, and then construct and solve the corresponding block of the secular equation:

free halothane and for the halothane-TMA complex are presented.

The off-diagonal terms of the secular equation are the matrix elements of the interaction of states determined by the Fermi resonances ($i, k = 2, 3$, and 4):

$$\begin{aligned}
 W_{1_ii} &= \frac{1}{2} \alpha_{1ii}, \\
 W_{1_ik} &= \frac{1}{2\sqrt{2}} \alpha_{1ik}
 \end{aligned} \quad (2)$$

Table 3. Spectroscopic parameters (MP2/6-311++G(d,p)) used in the calculation of resonance multiplets

Parameter	Monomer	Complex	Parameter	Monomer	Complex	Parameter	Monomer	Complex
ω_1	3185.5	3036.9	α_{134}	39.8	-44.1	x_{12}^0	-29.6	-29.9
ω_2	1365.5	1424.3	α_{144}	240.4	235.7	x_{13}^0	-6.3	-4.0
ω_3	1306.0	1310.3	β_{1123}	-46.7	-30.0	x_{14}^0	-56.4	-41.9
ω_4	1259.1	1339.9	β_{1124}	-32.7	-19.4	x_{22}^0	-0.7	-0.7
α_{111}	-327.8	-346.0	β_{1134}	-19.6	25.4	x_{23}^0	-3.8	-4.8
α_{122}	147.8	177.6	β_{2233}	4.0	1.6	x_{24}^0	-1.0	-3.1
α_{123}	60.3	34.8	β_{2244}	11.7	12.4	x_{33}^0	-5.4	-5.3
α_{124}	58.1	33.2	β_{3344}	0.45	-0.2	x_{34}^0	-0.9	-1.2
α_{133}	5.2	1.25				x_{44}^0	4.2	-0.2

and Darling–Dennison resonances. Complete expressions for the interaction matrix elements are given in [21]. Approximate expressions, which contain only the terms giving the maximum contributions, are given below:

$$W_{ii_{ik}} = \frac{1}{2\sqrt{2}} \left\{ \beta_{11ik} - \frac{1}{4} \alpha_{1ii} \alpha_{1ik} \left(\frac{1}{\omega_1 - 2\omega_i} + \frac{1}{\omega_1 - \omega_i - \omega_k} \right) - \frac{(3\alpha_{111} + \alpha_{1kk}) \alpha_{1ik}}{\omega_1} \right\},$$

$$W_{ik_{ij}} = \frac{1}{4} \left\{ \beta_{11kj} - \frac{1}{4} \alpha_{1ik} \alpha_{1ij} \left(\frac{1}{\omega_1 - \omega_i - \omega_k} + \frac{1}{\omega_1 - \omega_i - \omega_j} \right) - \frac{3(\alpha_{111} + 2\alpha_{1ii}) \alpha_{1kj}}{\omega_1} \right\}, \quad (3)$$

$$W_{ii_{kk}} = \frac{1}{2} \left\{ \beta_{iikk} - \frac{1}{4} \alpha_{1ii} \alpha_{1kk} \left(\frac{1}{\omega_1 - 2\omega_i} + \frac{1}{\omega_1 - 2\omega_k} \right) - \frac{\alpha_{1ik}^2}{2\omega_1} \right\}.$$

The secular equation in numerical form for the monomer:

$$\begin{array}{l} \langle 1000 | \\ \langle 0200 | \\ \langle 0110 | \\ \langle 0101 | \\ \langle 0020 | \\ \langle 0011 | \\ \langle 0002 | \end{array} \left\| \begin{array}{ccccccc} 3016.4 & 73.9 & 21.3 & 20.5 & 2.6 & 14.1 & 120 \\ & 2778.3 & -14.8 & -8.3 & 1.3 & 0 & -10.8 \\ & & 2692.7 & -5.4 & -11.6 & -4.4 & 0 \\ & & & 2668.4 & 0 & -14.3 & -9.3 \\ & & & & 2602.5 & -3.3 & -0.5 \\ & & & & & 2585.3 & -5.9 \\ & & & & & & 2567.6 \end{array} \right. \quad (4)$$

For the complex:

$$\begin{array}{l} \langle 1000 | \\ \langle 0200 | \\ \langle 0110 | \\ \langle 0101 | \\ \langle 0020 | \\ \langle 0011 | \\ \langle 0002 | \end{array} \left\| \begin{array}{ccccccc} 2841.5 & 88.8 & 12.3 & 11.7 & 0.6 & -15.6 & 118 \\ & 2778.3 & -12.1 & -7.5 & 0.5 & 0 & -36.3 \\ & & 2664.6 & 5.9 & -7.4 & -1.5 & 0 \\ & & & 2693.4 & 0 & -8.0 & -7.3 \\ & & & & 2548.6 & 4.6 & -0.5 \\ & & & & & 2585.1 & 9.5 \\ & & & & & & 2613.0 \end{array} \right. \quad (5)$$

As a result of diagonalization of the secular equation, the following solutions are obtained.

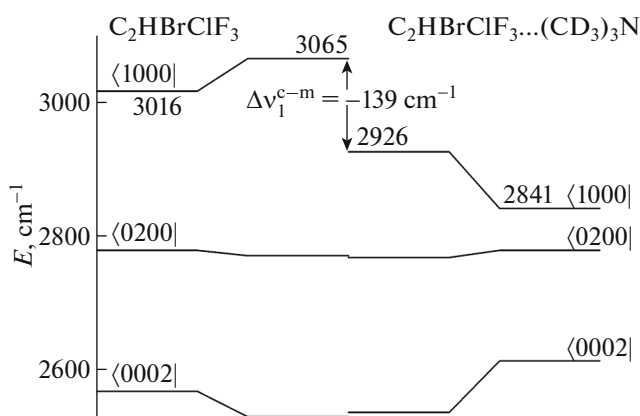


Fig. 5. The level diagram of resonance multiplets in the ν_1 region of free halothane and halothane-TMA complex.

Perturbed frequencies (wavenumbers) for the monomer (in cm^{-1}):

$$\begin{aligned} E_1(\nu_1) &= 3065.0, & E_2(2\nu_2) &= 2770.3, \\ E_3(\nu_2 + \nu_3) &= 2691.8, & E_4(\nu_2 + \nu_4) &= 2668.8, \\ E_5(2\nu_3) &= 2601.8, & E_6(\nu_3 + \nu_4) &= 2584.2, \\ E_7(2\nu_4) &= 2529.5. \end{aligned}$$

Perturbed frequencies for the complex (in cm^{-1}):

$$\begin{aligned} E_1(\nu_1) &= 2925.6, & E_2(2\nu_2) &= 2767.7, \\ E_3(\nu_2 + \nu_3) &= 2662.7, & E_4(\nu_2 + \nu_4) &= 2695.5, \\ E_5(2\nu_3) &= 2548.2, & E_6(\nu_3 + \nu_4) &= 2588.4, \\ E_7(2\nu_4) &= 2535.9. \end{aligned}$$

The diagram of the perturbed and unperturbed levels for the monomer and for the complex is shown in Fig. 5. The difference between the levels unperturbed by the resonance for the monomer and the complex is 75 cm^{-1} , and taking into account the resonance $\nu_1^c - \nu_1^m = -139 \text{ cm}^{-1}$, which is close to the experimental value (-136 cm^{-1}).

Wave functions for the monomer:

$$\begin{aligned} \psi_1 &= 0.945\langle 1000| + 0.232\langle 0200| + 0.044\langle 0110| \\ &\quad + 0.037\langle 0101| + 0.005\langle 0020| \\ &\quad + 0.023\langle 0011| + 0.222\langle 0002|, \\ \psi_2 &= -0.181\langle 1000| + 0.940\langle 0200| - 0.226\langle 0110| \\ &\quad - 0.087\langle 0101| + 0.021\langle 0020| \\ &\quad + 0.003\langle 0011| - 0.154\langle 0002|, \\ \psi_3 &= -0.061\langle 1000| + 0.176\langle 0200| + 0.923\langle 0110| \\ &\quad - 0.310\langle 0101| - 0.119\langle 0020| \\ &\quad + 0.002\langle 0011| - 0.051\langle 0002|, \end{aligned}$$

$$\begin{aligned} \psi_4 &= -0.042\langle 1000| + 0.122\langle 0200| + 0.273\langle 0110| \\ &\quad + 0.927\langle 0101| - 0.038\langle 0020| \\ &\quad - 0.169\langle 0011| - 0.139\langle 0002|, \end{aligned} \quad (6)$$

$$\begin{aligned} \psi_5 &= -0.006\langle 1000| + 0.004\langle 0200| + 0.115\langle 0110| \\ &\quad - 0.031\langle 0101| + 0.971\langle 0020| \\ &\quad - 0.205\langle 0011| + 0.008\langle 0002|, \end{aligned}$$

$$\begin{aligned} \psi_6 &= 0.024\langle 1000| - 0.013\langle 0200| + 0.059\langle 0110| \\ &\quad + 0.132\langle 0101| + 0.198\langle 0020| \\ &\quad + 0.942\langle 0011| - 0.227\langle 0002|, \end{aligned}$$

$$\begin{aligned} \psi_7 &= -0.261\langle 1000| + 0.125\langle 0200| + 0.057\langle 0110| \\ &\quad + 0.131\langle 0101| + 0.030\langle 0020| \\ &\quad + 0.203\langle 0011| + 0.924\langle 0002|. \end{aligned}$$

Wave functions for the complex:

$$\begin{aligned} \psi_1 &= 0.853\langle 1000| - 0.445\langle 0200| + 0.020\langle 0110| \\ &\quad + 0.022\langle 0101| + 0.001\langle 0020| \\ &\quad + 0.032\langle 0011| - 0.268\langle 0002|, \end{aligned}$$

$$\begin{aligned} \psi_2 &= 0.300\langle 1000| + 0.839\langle 0200| + 0.141\langle 0110| \\ &\quad + 0.103\langle 0101| - 0.007\langle 0020| \\ &\quad + 0.010\langle 0011| - 0.420\langle 0002|, \end{aligned}$$

$$\begin{aligned} \psi_3 &= -0.018\langle 1000| - 0.065\langle 0200| + 0.160\langle 0110| \\ &\quad + 0.970\langle 0101| - 0.010\langle 0020| \\ &\quad + 0.083\langle 0011| + 0.151\langle 0002|, \end{aligned}$$

$$\begin{aligned} \psi_4 &= -0.029\langle 1000| - 0.080\langle 0200| + 0.972\langle 0110| \\ &\quad - 0.184\langle 0101| - 0.063\langle 0020| \\ &\quad + 0.010\langle 0011| + 0.101\langle 0002|, \end{aligned} \quad (7)$$

$$\begin{aligned} \psi_5 &= 0.090\langle 1000| + 0.093\langle 0200| - 0.049\langle 0110| \\ &\quad - 0.103\langle 0101| - 0.098\langle 0020| \\ &\quad + 0.952\langle 0011| + 0.232\langle 0002|, \end{aligned}$$

$$\begin{aligned} \psi_6 &= 0.085\langle 1000| + 0.061\langle 0200| + 0.047\langle 0110| \\ &\quad - 0.023\langle 0101| + 0.976\langle 0020| \\ &\quad + 0.043\langle 0011| + 0.178\langle 0002|, \end{aligned}$$

$$\begin{aligned} \psi_7 &= 0.408\langle 1000| + 0.274\langle 0200| - 0.069\langle 0110| \\ &\quad - 0.063\langle 0101| - 0.183\langle 0020| \\ &\quad - 0.289\langle 0011| + 0.796\langle 0002|. \end{aligned}$$

Assuming zero own intensity of the overtones bands, the intensities of the components of the resonance multiplet can be calculated by the formula $I_k = I_0 b_{k1}^2$, where I_0 is the intensity of the ν_1 (CH) band in the harmonic approximation.

For the monomer $I_0 = 3.5 \text{ km/mol}$, for the complex $I_0 = 358 \text{ km/mol}$, b_{k1} are the coefficients at the vector $\langle 1000|$ in wave functions (6), (7).

Below are the intensities of the perturbed absorption bands of the complex (km/mol) estimated in this way: $I(\nu_1) = 261$, $I(2\nu_2) = 32$, $I(\nu_2 + \nu_4) = 0.12$, $I(\nu_2 + \nu_3) = 0.3$, $I(\nu_3 + \nu_4) = 2.9$, $I(2\nu_3) = 2.6$, $I(2\nu_4) = 60$. Three bands with noticeable intensity are observed experimentally. These are ν_1 , $2\nu_2$, and $2\nu_4$. It is their parameters that are shown in the far right side of the Table 2 (columns Fermi + D–D). It can be seen that the result obtained with full consideration of all possible resonance interactions $(\nu_1/2\nu_2/(\nu_2 + \nu_4)/(\nu_2 + \nu_3)/2\nu_4/(\nu_4 + \nu_3)/2\nu_3)$, practically correctly reflects the experimentally observed relative intensity distribution between the main band and two satellites. The absolute values of the obtained wavenumbers of the bands are expected to be somewhat overestimated, which is a general drawback of calculations at the MP2 level with valence-split Pople bases of the middle level. Nevertheless, their relative position is consistent with that observed in the experiment.

In the case of TMA, the predicted and measured changes in the frequencies of fundamental vibrations are in good agreement even in the harmonic approximation (Table 2). In conclusion, it should be noted that heavy halogens, chlorine and especially bromine, of halothane can potentially participate in binding with a target, in this case with TMA, through the formation of a so-called halogen bond. Preliminary calculations showed that the strength of such complexes is noticeably lower, and their formation was not detected in the framework of the spectroscopic experiments performed. The search for the conditions for the formation of complexes with a halogen bond is the subject of further research.

CONCLUSIONS

From the nature of changes in the IR absorption spectrum in liquid krypton, it can be concluded that halothane with TMA forms complexes with HB, which is characterized by a noticeable low-frequency shift of the donor's CH stretching vibration band. The absolute intensity of this band increases strongly. The appearance of intense satellites from the low-frequency side of the CH band is determined by strong resonant interactions with a pair of bending vibration overtones δ (CCH) and γ (CCH).

ACKNOWLEDGMENTS

Measurements and calculations were carried out using the equipment of the resource centers of the St. Petersburg State University (SPbSU): Geomodel, Applied Aerodynamics and RVCV (<http://cc.spbu.ru>).

FUNDING

This work was carried out with the support of the Russian Foundation for Basic Research, project no. 20-03-00536.

CONFLICT OF INTEREST

The authors declare that they have no conflict of interest.

REFERENCES

1. B. Michielsen, W. A. Herrebout, and B. J. van der Veken, *ChemPhysChem* **9**, 1693 (2008).
2. B. Michielsen, W. A. Herrebout, and B. J. van der Veken, *ChemPhysChem* **8**, 1188 (2007).
3. S. M. Melikova, K. S. Rutkovskii, and M. Rospenk, *Opt. Spectrosc.* **123**, 30 (2017).
4. B. Michielsen, J. J. Dom, B. J. van der Veken, S. Hesse, Xue Zhifeng, M. A. Suhm, and W. A. Herrebout, *Phys. Chem. Chem. Phys.* **12**, 14034 (2010).
5. K. S. Rutkowski, W. A. Herrebout, S. M. Melikova, P. Rodziewicz, B. J. van der Veken, and A. Koll, *Spectrochim. Acta, A* **61**, 1595 (2005).
6. W. A. Herrebout, S. M. Melikova, S. N. Delanoye, K. S. Rutkowski, D. N. Shchepkin, and B. J. van der Veken, *J. Phys. Chem. A* **109**, 3038 (2005).
7. K. S. Rutkowski, A. Karpfen, S. M. Melikova, W. A. Herrebout, A. Koll, P. Wolschann, and B. J. van der Veken, *Phys. Chem. Chem. Phys.* **11**, 1551 (2009).
8. S. M. Melikova, K. S. Rutkowski, P. Rodziewicz, and A. Koll, *Chem. Phys. Lett.* **352**, 335 (2002).
9. K. Hermansson, *J. Phys. Chem. A* **106**, 4695 (2002).
10. K. S. Rutkowski, P. Rodziewicz, S. M. Melikova, W. A. Herrebout, B. J. van der Veken, and A. Koll, *Chem. Phys.* **313**, 225 (2005).
11. B. J. van der Veken, *J. Phys. Chem. A* **100**, 17436 (1996).
12. M. J. Frisch, G. W. Trucks, H. B. Schlegel, G. E. Scuseria, M. A. Robb, J. R. Cheeseman, G. Scalmani, V. Barone, G. A. Petersson, H. Nakatsuji, X. Li, M. Caricato, A. V. Marenich, J. Bloino, B. G. Janesko, et al., *Gaussian 16, Revision A.03* (Gaussian Inc., Wallingford CT, 2016).
13. C. Möller and M. S. Plesset, *Phys. Rev.* **46**, 618 (1934).
14. R. G. Parr and W. Yang, *Density-Functional Theory of Atoms and Molecules* (Oxford Univ. Press, New York, 1989).
15. S. F. Boys and F. Bernardy, *Mol. Phys.* **19**, 53 (1970).
16. S. Simon, M. Duran, and J. J. Dannenberg, *J. Chem. Phys.* **105**, 11024 (1996).
17. B. T. Darling and D. M. Dennison, *Phys. Rev.* **57**, 128 (1940).
18. W. F. Murphy, F. Zerbetto, J. L. Duncan, and D. C. McKean, *J. Phys. Chem.* **97**, 581 (1993).
19. B. Czarnik-Matusiewicz, D. Michalska, C. Sandorfy, and Th. Zeegers-Huyskens, *Chem. Phys.* **322**, 331 (2006).
20. I. M. Mills, in *Molecular Spectroscopy: Modern Research*, Ed. by K. N. Rao and C. W. Mathews (Academic, New York, 1972), p. 115.
21. A. M. Rosnik and W. F. Polik, *Mol. Phys.* **112**, 261 (2014).

Translated by N. Petrov